Physicochemical properties of divinyl chlorophylls *a*, *a'* and divinyl pheophytin *a* compared with those of monovinyl derivatives

Hirohisa Komatsu[1], Daiki Fujinuma[1], Shinya Akutsu[1], Daisuke Fukayama[1], Yuhta Sorimachi[1], Yuki Kato[2], Yoshinori Kuroiwa[2], Tadashi Watanabe[3], Hideaki Miyashita[4], Koji Iwamoto[5], Yoshihiro Shiraiwa[5], Mayumi Ohnishi-Kameyama[6], Hiroshi Ono[6], Hiroyuki Koike[7], Mayumi Sato[8], Masanobu Kawachi[8], Masami Kobayashi[1]*

[1]*Division of Materials Science, Faculty of Pure and Applied Science, University of Tsukuba, Tsukuba, Ibaraki, 305-8573, Japan*
[2] *Institute of Industrial Science, University of Tokyo, Tokyo 153-8505, Japan*
[3]*Research Center for Math and Science Education, Organization for Advanced Education, Tokyo University of Science, Tokyo 162-8601, Japan*
[4]*Graduate School of Human and Environment Studies, Kyoto University, Kyoto 606-8501, Japan*
[5]*Faculty of Life and Environmental Sciences, University of Tsukuba, Japan*
[6]*National Food Research Institute, Tsukuba 305-8642, Japan*
[7]*Department of Biological Sciences, Faculty of Science and Engineering, Chuo University, Tokyo 112-8551*
[8]*National Institute for Environmental Studies, Ibaraki 305-8506, Japan*

(*Corresponding author e-mail: masami@ims.tsukuba.ac.jp)

Precise physicochemical properties of divinyl chlorophylls were compared with those of monovinyl Chls. Divinyl Chl *b* was clearly separated from monovinyl Chl *b* by a normal-phase HPLC with isocratic eluent mode, and pairs of DV- and MV-Chls *a*, *a'*, and pheophytins *a* were well separated by a reversed-phase HPLC also with isocratic eluent mode. Absorption spectra of DV-Chls were practically similar to those of monovinyl ones, while the former showed the red-shifted Soret band and the slightly reduced Q_Y band. Circular dichroism spectra of DV- and MV-Chls also exhibited almost the same spectra, although the intensity of the former was a little small. Precise mass and NMR spectra of DV- and MV-Chls were performed for the first time. The first oxidation and reduction potentials of DV-Chl *a* were for the first time clarified to be very slightly more positive than those of MV-Chl *a* by 8 mV and 10 mV, respectively.

Introduction

Chlorophylls are essential molecules in oxygenic photosynthesis, and chlorophyll (Chl) *a* (monovinyl Chl *a*, MV-Chl *a*: Fig. 1) is the major chlorophyll in cyanobacteria, algae and terrestrial plants. Primary charge separation is initiated by a few specially-tailored chlorophylls in the reaction centers (RCs); *e.g.*, the 13^2-epimer of Chl *a*, Chl *a'* (MV-Chl *a'*; Fig. 1), constitutes the primary electron donor of P700 in PS I as a heterodimer of Chl *a/a'* (Kobayashi *et al.* 1988; Jordan *et al.* 2001), and a metal-free Chl *a*, pheophytin (Phe) *a* (MV-Phe *a*; Fig. 1), functions as the primary electron acceptor in PS II (Klimov *et al.* 1977a,b; Zouni *et al.* 2001).

In 1983, an unfamiliar chlorophyll which had the absorption maxima 436 and 661 nm in diethyl ether was isolated from the fractions with the particles of less-than-one μm in surface waters of the tropical Atlantic Ocean (Gieskes and Kraay 1983, 1986), and its absorption spectrum was identical to that of divinyl Chl *a* (DV-Chl *a*; Fig. 1) purified from a mutant of *Zea mays* (Bazzaz 1981; Bazzaz and Brereton 1982). In 1988, a free-living marine prochlorophyte, *Prochlorococcus marinus*, was discovered in seawater samples (Chisholm *et al.* 1988), and the cells were found to be smaller than common cyanobacteria and contain DV-Chl *a* characterized by a red-shift of the Soret peak by 8-10 nm compared to normal Chl *a* (MV-Chl *a*).

The chemotaxonomic assessment of phytoplankton populations in natural waters requires good biochemical markers, and DV-Chl *a* is a good marker for *Prochlorococcus*, because no other wild-type photooxytroph having this pigment is known. The numerical abundance of *Prochlorococcus* is usually very high relative to other phytoplankton, and DV-Chl *a* contributes up to 40% to total Chl *a* (the sum of MV-Chl *a* and DV-Chl *a*) (Goericke and Repeta 1993; Letelier *et al.* 1993; Bidigare and Ondrusek 1996); *Prochlorococcus* is estimated to contributes more than 50% to total phytoplankton pigment biomass (Campbell *et al.* 1994). The spectrophotometric or fluorometric measurements of total Chl *a* resulted in biased estimation of total Chl *a* for seawater samples due to the spectral differences between MV-Chl *a* and DV-Chl *a* (*e.g.*, Jeffrey and Humphrey 1975). Their co-elution on HPLC traces also led to a significant overestimation (15-25%) of total Chl *a* (Goericke and Repeta 1993; Letelier *et al.* 1993; Latasa *et al.* 1996), and hence the separation of DV-Chl *a* from MV-Chl *a* to avoid the overestimation has been recommended and challenged for a considerable time (see Zapata *et al.* 2000; Jayaraman *et al.* 2011).

In 2012, we have achieved, for the first time,

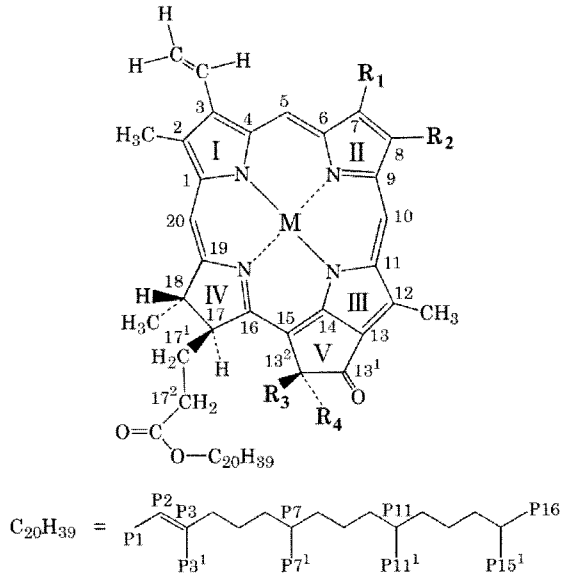

	M	R_1	R_2	R_3	R_4
Chl *a*	Mg	CH_3	CH_2CH_3	H	$COOCH_3$
Chl *a'*	Mg	CH_3	CH_2CH_3	$COOCH_3$	H
Phe *a*	2H	CH_3	CH_2CH_3	H	$COOCH_3$
Phe *a'*	2H	CH_3	CH_2CH_3	$COOCH_3$	H
DV-Chl *a*	Mg	CH_3	$CH=CH_2$	H	$COOCH_3$
DV-Chl *a'*	Mg	CH_3	$CH=CH_2$	$COOCH_3$	H
DV-Phe *a*	2H	CH_3	$CH=CH_2$	H	$COOCH_3$
DV-Phe *a'*	2H	CH_3	$CH=CH_2$	$COOCH_3$	H
DV-Chl *b*	Mg	CHO	$CH=CH_2$	H	$COOCH_3$

Fig. 1 Molecular structure and carbon numbering of chlorophylls, according to the IUPAC numbering system.

the separation of DV-Chls from MV-Chls on a C22-based reversed-phase HPLC column with isocratic mode, and found that *Prochlorococcus* sp. NIES-3376 possessed DV-Chl *a'* and DV-Phe *a*, instead of MV-Chl *a'* and MV-Phe *a*, as minor key components in the RCs, as well as the major DV-Chls *a* and *b*.

To date, however, there is only scarce information on physicochemical properties of DV-Chl derivatives, most probably due to the difficulties in (1) mass cultivation of *Prochlorococcus* and (2) the separation of DV-Chls from MV-Chls. In this paper, we present essential physicochemical properties of DV-Chl *a* prepared from an *slr1923*-inactivated mutant of *Synechocystis* 6803 producing DV-Chl *a* (Islam *et al.* 2008) and its derivatives comparing with MV-ones *in vitro*, introducing the experimental procedures of HPLC, absorption, circular dichroism (CD), mass, NMR spectra and redox potentials.

Materials and methods

Algal culture

Culture strain of *Prochlorococcus* sp. (NIES-3376) was maintained in the Microbial Culture Collection at the National Institute for Environmental Studies. The NIES-3376 strain for the analysis was cultivated in PRO99 medium (Moore *et al.* 2002) at 295 K and illuminated with 5 μmol photon m^{-2} s^{-1} of white fluorescence light using a 10:14-h light:dark cycle. The PRO99, seawater based medium, was prepared with the natural oligotrophic seawater collected from the Pacific Ocean (33.201N, 139.471E, 3-5 m depth). An *slr1923*-inactivated mutant of *Synechocystis* 6803 producing DV-Chl *a* was cultured as described elsewhere (Islam *et al.* 2008)

Pigment preparation

MV-Chl *a* and MV-Chl *b* were extracted with acetone/methanol (7/3, *v/v*) mixture at 277 K from parsley (*Petroselinum crispum* Nym.). DV-Chl *a* was extracted from the *slr1923*-inactivated mutant of *Synechocystis* 6803. The extract was applied to a preparative-scale normal-phase HPLC (Senshupak 5251-N, 250 mm x 20 mm i.d.) and eluted with hexane/2-propanol/methanol (100/2/0.4, *v/v/v*) at a flow rate of 7 mL min^{-1} at 277 K, as described elsewhere (Kobayashi *et al.* 1991). Other pigment standards, MV-Chl *a'*, MV-Phe *a/a'*, DV-Chl *a'* and DV-Phe *a/a'*, were prepared by epimerization and acidification of authentic MV-Chl *a* and DV-Chl *a* as described elsewhere (Watanabe *et al.* 1984).

HPLC analysis

Pigments were extracted from *Prochlorococcus* sp. NIES-3376 cell pellet (ca. 10 μL) with sonication in a ca. 300-fold volume of acetone/methanol (7/3, *v/v*) mixture for 2 min in the dark at 277K. The extract was filtered and dried in vacuo. The whole procedure was completed within 5 min. The solid material thus obtained was immediately dissolved in ca. 10 μL of chloroform. Reversed-phase HPLC analysis was performed by a C22-based column (Senshupak DOCOSIL SP100, 250 x 4.6 mm i.d.) cooled to 277 K in an ice-water bath; the pigments were eluted isocratically with degassed ethanol/methanol/2-propanol (86/13/1, *v/v/v*) at a flow rate of 1.4 mL min^{-1}, and were monitored with a JASCO UV-2070 detector (λ = 665 nm) and a SHIMADZU Multiwavelength SPD-M10A VP photodiode array detector (λ = 300 - 800 nm) in series. Normal-phase HPLC analysis was performed by a silica column (YMC-pak SIL, 250 x 4.6 mm i.d.) cooled to 277 K in an ice-water bath; the pigments were eluted isocratically with degassed hexane/2-propanol/methanol (100/0.7/0.2, *v/v/v*) at a flow rate of 0.9 mL min^{-1}, and were monitored with a JASCO UV-970 detector (λ = 665 nm) and a JASCO Multiwavelength MD-915 detector (λ = 300 - 800 nm) in series.

Visible absorption spectra

Visible absorption spectra of the Chl solutions were recorded on a JASCO spectrophotometer Model V-560 at room temperature. Reagent-grade diethyl ether, acetone, methanol and benzene were used as received.

Circular dichroism spectra

A spectropolarimeter Model FDCD-309 (JASCO) was used for CD measurements. Benzene was chosen as

the solvent, in view of the sufficiently slow interconversion between epimeric species in this medium (Watanabe *et al.* 1984). The spectra were recorded from 800 nm to 300 nm at a scan rate of 200 nm/min with 20 scans at room temperature; time for measurement was ca. one hour.

Mass spectra

LC/MS experiments were performed on an LCQ mass spectrometer (Thermo Fisher Scientific Inc., MA, U.S.A.) equipped with an HPLC system (HP1100, Agilent, CA, U.S.A.) connected with a diode array detector. Each sample dissolved in dichloromethane before analysis was applied on a JASCO Finepak SIL C18S column (150 mm x 4.6 mm i.d.) cooled to 277 K in an ice-water bath, and separated using a mixture of ethanol/methanol/2-propanol/water (86/13/1/3, *v/v*) at a flow rate of 300 μL min^{-1}. The eluate was monitored by the UV-Vis spectrum in a range of 220-800 nm, and was introduced into the mass spectrometer from 5 to 55 min after sample injection. Atmospheric pressure chemical ionization (APCI) mass and MS/MS spectra were recorded in the positive-ion mode in the mass range of *m/z* 150-2,000. Helium was used as collision gas for MS/MS experiments, followed by the isolation of ions over a selected mass window of 2 Da. The mass spectrometer was initially tuned using a standard Chl *a* solution as follows: APCI vaporizer temp., 723 K; spray voltage, 4 kV; capillary temperature, 423 K; capillary voltage, 8 V; sheath gas (nitrogen) flow rate, 56 (arbitrary unit); auxiliary gas flow rate, 9 (arbitrary unit).

Nuclear magnetic resonance spectra

The nuclear magnetic resonance (NMR) spectra were recorded on a Bruker Avance 800 spectrometer (Bruker Biospin, Karlsruhe, Germany), with a frequency of ^{1}H at 800 MHz and ^{13}C at 201 MHz, equipped with TCI CryoProbe using a microtube (Shigemi Inc., Tokyo) and about 0.5 mg of sample in 0.3 mL of acetone-d_6 with tetramethylsilane (TMS) as an internal standard. The chemical shifts are given in δ-scale [ppm] downfield from TMS. The measurements were performed at 273 K. The typical experimental conditions for the ^{1}H NMR spectra were 256 scans, a spectral width of 17 ppm, 128K data points. The ^{13}C spectra were acquired using a power gated decoupling with 48k scans. The spectral width of 220 ppm was acquired in 64 K data points. The 2D-homonuclear (Nuclear Overhauser and Exchange Spectroscopy (NOESY)) and 2D-heteronuclear (H,C-Heteronuclear Single Quantum Coherence (H,C-HSQC) and H,C-Heteronuclear Multiple Bond Correlation (H,C-HMBC)) experiments were performed for the structural assignments of the ^{1}H and ^{13}C signals using standard 2D-NMR pulse sequences of Bruker software.

Electrochemical measurement

The measurements were performed with an ALS model 620A electrochemical analyzer. Parameters for square wave voltammetry (SWV) were V_{step} = 5.0 mV, AC signal (V_{pulse}) = 25 mV, and p-p at 8 Hz. The measurements were carried out in an air-tight electrochemical cell containing small compartment for a sample solution equipped with a glass filter that can be degassed and filled with dry N_2. A platinum disk electrode with 1.6 mm in diameter (outer diameter: 3 mm) was used as the working electrode, and a platinum black wire fabricated in the small compartment (internal diameter: 8.9 mm) as the counter electrode. An Ag/AgCL electrode, chosen for good reproducibility despite possibility of junction potential, was connected through a salt bridge to the outer electrolytic solution of the small components. The ferrocene-ferrocinium redox couple was used to estimate junction potential changes upon changing solvents. After each measurement, the redox potentials of the ferrocene-ferrocinium were measured as +0.45 V vs. Ag/AgCL in acetonitrile.

Results and discussion

HPLC

Typical isocratic normal-phase high performance liquid chromatography (HPLC) traces for acetone/methanol extract from cells of *Prochlorococcus* sp. NIES-3376 and pigment standard (MV-Phe *a*, Chl *a'*, Chl *a*, Chl *b'*,Chl *b*; DV-Phe *a*, Chl *a'*, Chl *a*) are shown in Figs. 2A and B, respectively. DV-Chl *b* and MV-Chl *b* were clearly separated even with isocratic eluent mode, while DV-Chl *a* and MV-Chl *a* were partially separated. Neither a primed pair (DV- and MV-Chls *a'*) nor metal-free Chls (DV- and MV-Phes *a*) were separated, whereas our system had been quite useful for the separation of mixture containing only MV-pigments (MV-Chls *a, a', b, b', d, d', f, f'*, MV-Phe *a, a', b, b', d, d', f, f'*)(Kobayashi *et al.* 2013) or only DV-pigments (DV- Chls *a, a', b,* DV-Phe *a, a', b*). Our normal-phase system is thus found to be unsuitable for the separation of MV-Phe *a* and DV-Phe *a* as well as MV-Chl *a'* and DV-Chl *a'*.

A typical isocratic reversed-phase HPLC trace for pigment standard (MV-Phe *a*, Chl *a'*, Chl *a*, Chl *b'*, Chl *b*; DV-Phe *a*, Chl *a'*, Chl *a*) is shown in Fig. 2D. Both a primed pair (DV- and MV-Chls *a'*) and a metal-free pair (DV- and MV-Phes *a*) were well separated even with simple isocratic eluent mode in a single run. DV-Chl *a* and MV-Chl *a* were also nicely separated, but only the resolution of DV-Chl *b* and MV-Chl *b* was poor. Our simple isocratic reversed-phased HPLC has been found to be selective enough to resolve DV-Chl *a,* the marker pigment for the prokaryote *Prochlorococcus,* from MV-Chl *a*.

In the late 1970s, the HPLC technique was applied to the separation of plant pigments. In many cases the reversed-phase HPLC was preferred (Eskins *et al.* 1977; Shoaf *et al.* 1978; Schoch 1978), and is still the main option to date. However, the separation by C18 column-based reversed-phase HPLC, commonly used for the analysis of phytoplankton

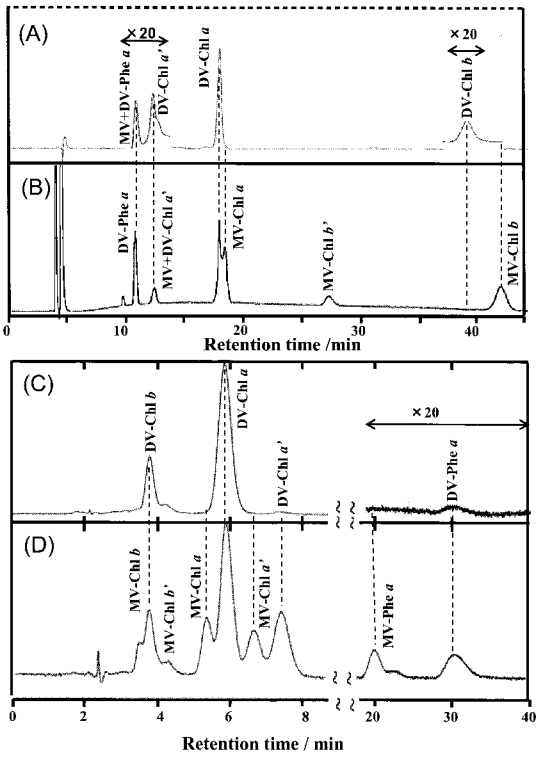

Fig. 2 Normal-phase (top) and reversed-phase (bottom) HPLC profiles for acetone/methanol extracts of *Prochlorococcus* sp. NIES-3376 (A, C) and a mixture of authentic MV-Chl *b*, MV-Chl *b'*, MV-Chl *a*, DV-Chl *a*, MV-Chl *a'*, DV-Chl *a'*, MV-Phe *a* and DV-Phe *a* (B, D). Detection wavelength is 665 nm.

pigments in seawater, has not been performed, and hence a reversed-phased C8 HPLC with binary or ternary solvent gradient has achieved the separation of MV-Chl *a* and DV-Chl *a* (Wright *et al.* 1991; Goericke and Repeta 1993; Zapata *et al.* 2000; Van Heukelem and Thomas 2001). For the separation of phytoplankton pigments, a reversed-phase C16-amide HPLC column incorporating a ternary gradient system is now recommended and widely used (Jayaraman *et al.* 2011, see also a review Jeffrey *et al.* 1999). However, the elution gradient for simultaneous separation of pigments is unfavorable for quantitative analysis, since the molar absorptivities of pigments strongly depend on solvents. In this context, the simple isocratic eluent systems with the combination of normal- and reversed-phase HPLC columns are favorable and powerful tool for assessing the distribution of the phytoplankton in marine and fresh water.

One should note that both MV-Chl *a'* and MV-Phe *a* were not detected at all in *Prochlorococcus sp.* NIES-3376, but both DV-Chl *a'* and DV-Phe *a* exit as the minor components in this picoplankton (Fig. 2C). In *Prochlorococcus* sp. NIES-3376, DV-Chl *a'* and DV-Phe *a* must function as the primary donor of PS I and the primary electron acceptor in PS II, respectively, instead of MV-Chl *a'* and MV-Phe *a* functioning in normal cyanobacterial reaction centers (Fujinuma *et al.* 2012).

Visible absorption spectra

Absorption spectra of DV-Chl *a* and MV-Chl *a* in four kinds of solvent measured at room temperature are illustrated in Figs. 3 (top) and 4A', B'; their spectral shapes were very similar to each other, except that MV-Chl *a* in methanol showed a broadening of the Soret band and its smaller intensity than that of Q_Y band. As compared to MV-Chl *a*, DV-Chl *a* showed the slightly but significantly red-shifted Soret band and the very small intensity reduction of Q_Y band, while little changes were seen in the Q_Y band wavelengths in all solvents examined here. The Qx exhibits practically no intensity.

Inductive effects on the absorption wavelengths and intensities of Soret bands and Q_Y bands of chlorophylls strongly depend on the nature and position of substituent(s) on the macrocycle (Gouterman 1961; Gouterman *et al.* 1963; Weiss 1978; Petke *et al.* 1979; Hanson 1991; Kobayashi *et al.* 2006, 2013). For example, replacement of the electron-donating group, $\leftarrow CH_3$, on ring II of Chl *a* by the electron-withdrawing group, $\rightarrow$CHO, yielding Chl *b*, causes remarkable red-shift of Soret band (ca. 25 nm) relative to Chl *a* and significantly strong intensity reduction of the Q_Y band (Kobayashi *et al.* 2013). A similar but weak tendency is seen in DV-Chl *a*, when a $\leftarrow CH_2{-}CH_3$ group on ring II of MV-Chl *a* is replaced with a $-CH{=}CH_2$ moiety, where the red-shift of Soret band was seen but smaller (ca. 7 nm), and the negligibly small intensity reduction of the Q_Y band was observed. The findings, however, indicate it is a general feature that substitution by the electron-withdrawing group on ring II causes the intensity reduction of the Q_Y band as well as the red-shift of the Soret band.

Pheophytins *a* possessed relatively strong and characteristic Q_X bands in the region of 490-550 nm in all solvents illustrated in Figs. 3 (bottom) and 4C', D'. The Q_X bands in MV-Phe *a* were well resolved to the Q_X (0,0) and Q_X (1,0) transitions. In contrast, the Q_x (0.0) band (longer wavelength) of DV-Phe *a* looks unclear. DV-Phe *a* also showed the red-shift of Soret band by ca. 10 nm and the very slight reduction of Q_Y band in intensity compared to MV-Phe *a*.

As mentioned above, we had better note that the Soret band of MV-Chl *a* in methanol looks broad, and the intensity of Sore band is smaller than that of Q_Y band, while such features were not seen in pheophytins. The broad Soret band may be caused by some interactions of the central metal, Mg, of MV-Chl *a* with (a) methanol molecule(s) or a neighboring MV-Chl *a* molecule, although further investigations are needed.

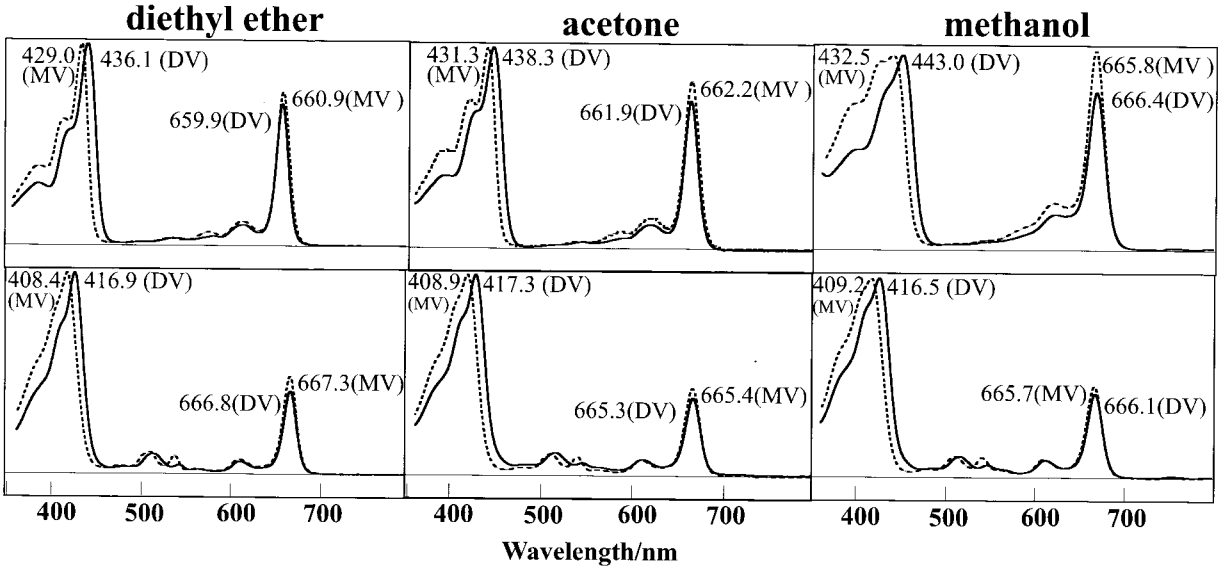

Fig. 3 Comparison of the absorption spectra of DV-Chl *a*/MV-Chl *a* (top) and DV-Phe *a*/MV-Phe *a* (bottom) in diethyl ether, acetone and methanol at room temperature. Spectra were scaled to the Soret-band maximum.

Circular dichroism spectra

Circular dichroism (CD) spectra are very useful for distinction between the primed chlorophyll, *e.g.*, Chl *a'*, and the corresponding non-primed one, Chl *a*, whereas the absorption characteristics of the primed derivatives (Chls *a'*, *b'*, *d'*, *f'*, Phes *a'*, *b'*, *d'* and *f'*) are practically identical with those of the non-primed ones (Wolf and Scheer 1973; Weiss 1978; Watanabe *et al.* 1984; Kobayashi *et al.* 2006, 2013).

The CD spectra of DV-Chl *a/a'*, MV- Chl *a/a'*, DV-Phe *a/a'* and MV-Phe *a/a'* as well as their absorption spectra in benzene at room temperature are illustrated in Fig. 4. For a given pair of epimers, the CD spectra as well as the absorption spectra look similar in shape to each other. For each of DV-Chl *a'* and MV-Chl *a'*, an intense negative CD associated with Q_Y (0,0) were clearly seen, while the intensity of DV-Chl *a'* (Fig. 4A) was a little weaker than that of MV-Chl *a'* (Fig. 4B). On the other hand, the non-primed species, DV-Chl *a* and MV-Chl *a*, showed complicated and very weak negative/positive activities at this transition (Figs. 4A, B). Note that the CD spectrum of DV-Chl *a* apparently reflect the existence of the two transitions: they showed a positive maximum and a negative minimum with the center wavelength roughly coinciding with its Q_Y absorption maximum. Each well-defined satellite peak associated with Q_Y (1,0) was weakly positive for DV-Chl *a'* but weakly negative for MV-Chl *a'*.

In contrast, all four pheophytins showed negative activities in the Q_Y (0,0) region, and primed ones revealed stronger and blue-shifted signals compared to the non-primed ones, although the negative peak of DV-Phe *a* was negligibly small, suggesting that the Q_Y maximum transition of Phes consists of at least two bands, where shorter wavelength band shows stronger activity in primed Phe and longer wavelength band stronger in non-primed Phe, especially in MV-Phe *a*. The well-defined satellite peak associated with Q_Y (1,0) was not seen in pheophytins (Figs. 4C, D).

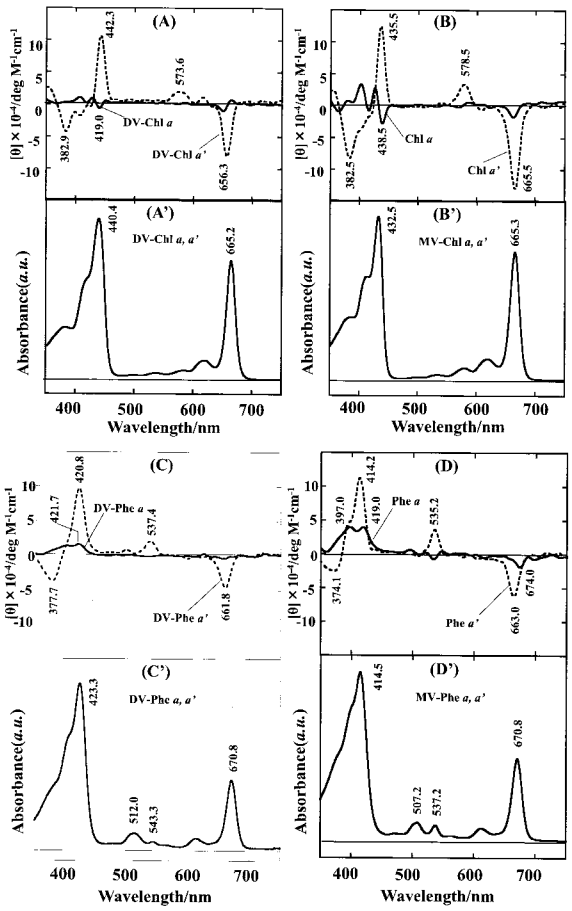

Fig. 4 CD spectra for (A) DV-Chls *a/a'*, (B) MV-Chls *a/a'*, (C) DV-Phes *a/a'*, (D) MV-Phes *a/a'*, and (A')-(D') the corresponding absorption spectra in benzene at room temperature. [θ] denotes the molar ellipticity.

A series of Q_X transitions occur in the "valley" of the absorption spectrum. The relatively strong positive CD activities of the non-primed ones derived from the Q_X (0,0) absorption (called band III; Petke *et al.* 1979) appeared at 574, 579, 537, 535 nm for DV-Chl *a'*, MV-Chl *a'*, DV-Phe *a'*, MV-Phe *a'*, respectively, while MV-Chl *a* and MV-Phe *a* exhibited a little complicated CD spectra, namely, negative/positive for MV-Chl *a* and positive/negative/positive for MV-Phe *a* in shape, respectively. DV-Chl *a* and DV-Phe *a* showed practically no intensity in this region. Note that although the absorption peak associated with Q_X (0,0) transition of DV-Phe *a'* (Fig. 4C') is very small as compared with that of MV-Phe *a'* (Fig. 4D'), but the corresponding CD signal of DV-Phe *a'* is strong enough to be clearly seen (Fig. 4C). The CD activity associated with the Q_X (0,1) absorption satellites (band IV) at the shorter wavelength was very weak.

The Soret bands of Chls and Phes contain many π-π^* transitions characterized by a complex mixture of configurations, and band B in the Soret absorption consists of two nearly degenerate electronic transitions, B_X (0,0) and B_Y (0,0) (Weiss 1978; Petke *et al.* 1979; Hanson 1991). All the primed derivatives gave single and strongly positive CD spectra at this absorption peak, and the two transitions contributed to the CD spectra in a similar manner as reported (Watanabe *et al.* 1984; Kobayashi *et al.* 2013). In contrast, the CD spectra of none-primed DV-Chl *a* and MV-Chl *a* reflected the existence of the clear two transitions in this region: they show a maximum and a minimum with the center wavelength roughly coinciding with the Soret absorption maximum, as seen in the CD spectrum of Q_Y-band in DV-Chl *a* as mentioned above. Primed Chls and Phes exhibited relatively intense negative CD spectra in the near ultraviolet at η-bands (Weiss 1978; Petke *et al.* 1979) of the Soret region, whereas non-primed ones exhibited positive activities. Note that these negative peak intensity of DV-Phe *a'* is stronger than that of MV-Phe *a'*. The positive CD spectra at η-bands of non-primed DV-ones were significantly weaker than that of non-primed MV-ones.

Relatively a little weaker CD intensity seen in DV-Chls and Phes in Fig. 4 may be caused by the configuration difference at C8 between DV- and MV-derivatives, because the C8-ethyl moiety in MV-Chl *a* was reported to be perpendicular to the ring plane, but the direction of the C8-vinyl side-chain was almost coplanar to the ring plane in DV-Chl *a*, based on the density functional theory (DFT) calculations (Tomo *et al.* 2009).

Mass spectra

As illustrated in Fig. 5A, MV-Chl *a* ($C_{55}H_{72}MgN_4O_5$, monoisotopic mass; 892.535. Hereafter the value in the bracket shows the monoisotopic mass of the molecule or the ion) gives the protonated molecule ($[M+H]^+$) at *m/z* 893.2 producing the dominant fragment ion at *m/z* 615.1, The mass difference 278 between $[M+H]^+$ and the product ion corresponds to $C_{20}H_{28}$. This suggests the presence of a phytyl chain in MV-Chl *a*. The other product ions at *m/z* 583.0 and *m/z* 555.2 corresponding to $[M+H-278-32]^+$ and $[M+H-278-60]^+$, respectively, are the results of the loss of carboxymethyl group followed by the cleavage of phytol. The losses of 278, 310 and 338 from the precursor ion in MS/MS spectra are seen in all the pigments examined here reveals the presence of *a* phytyl chain. Similar features were observed in DV-Chl *a* ($C_{55}H_{70}MgN_4O_5$, 890.520) (Fig. 5B), though all the observed values are 2 Da smaller than those observed in MV-Chl *a*, due to the replacement of $-CH_2CH_3$ with $-CH{=}CH_2$ in DV-Chl *a*. MV-Phe *a* and DV-Phe *a* showed the similar patterns (Figs. 5C and D).

As seen in Figs. 5C, D, the corresponding pheophytins showed the absence of magnesium, Mg, *e.g.*, $[M+H]^+$ of DV-Phe *a* is observed at *m/z* 869.4 which is 22 Da smaller than that of DV-Chl *a*, showing the substitution of Mg with two H atoms in DV-Phe *a*.

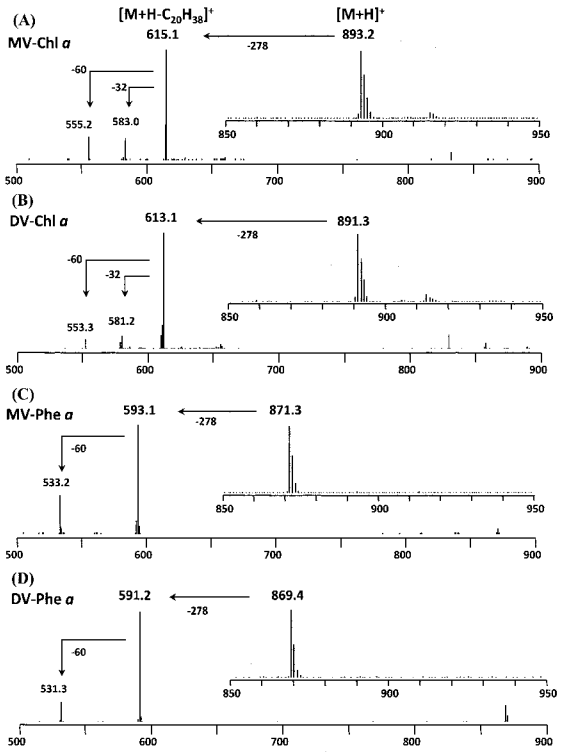

Fig. 5 MS/MS spectra of (A) MV-Chl *a*, (B) DV-Chl *a*, (C) MV-Phe *a* and (D) DV-Phe *a*. Each mass spectrum of the chlorophyll fraction is shown in the shaded square. MS/MS spectra of the protonated molecules ($[M+H]^+$) of MV- and DV-Chls *a* give product ions of $[M+H-278]^+$, $[M+H-278-32]^+$ and $[M+H-278-60]^+$. MV- and DV-Phes *a* give product ions of $[M+H-278]^+$ and $[M+H-278-60]^+$.

Nuclear magnetic resonance spectra

A: ^{1}H-NMR

As observed in one-dimensional ^{1}H-NMR spectra (Fig. 6, Table 1), marked differences are seen in the signals arising from the ethyl and vinyl groups. Two high-field signals characteristic of the ethyl group observed at 3.817 ppm (q, 8^1-H) and 1.696 ppm (t, 8^2-

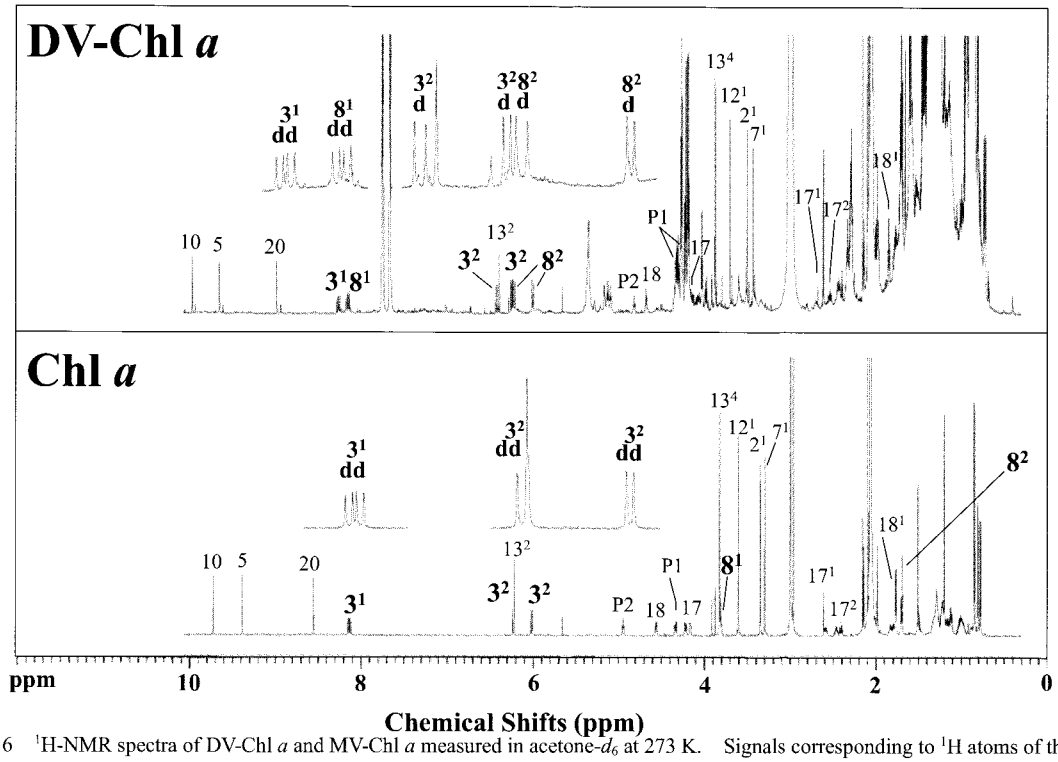

Fig. 6 ^{1}H-NMR spectra of DV-Chl *a* and MV-Chl *a* measured in acetone-d_6 at 273 K. Signals corresponding to ^{1}H atoms of the macrocycle are labeled with the numbers of the corresponding carbons. The peak at 2.06-2.11 ppm is acetone and 3.07-3.10 ppm is H_2O, respectively.

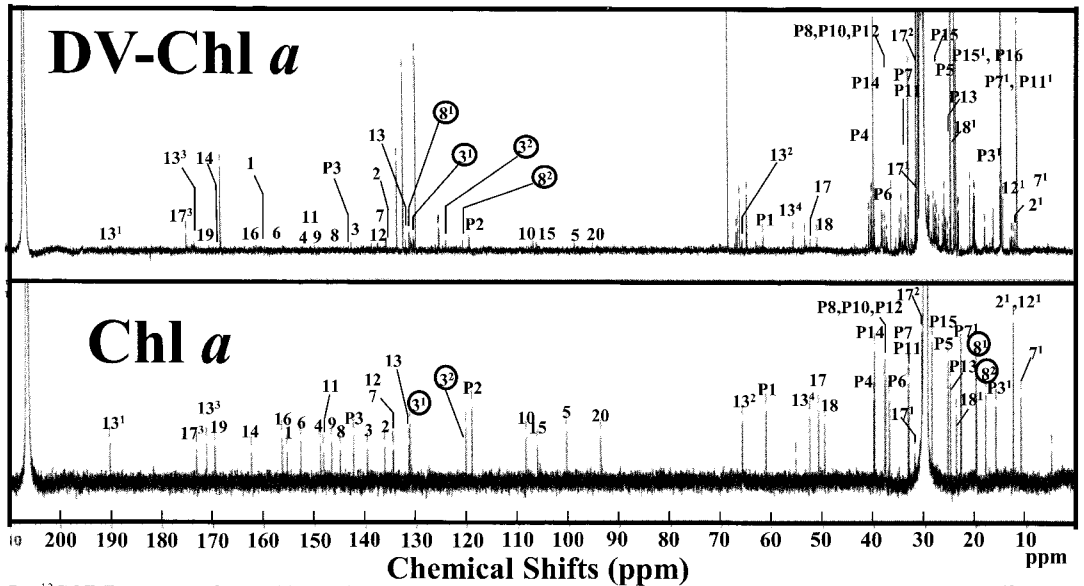

Fig. 7 ^{13}C-NMR spectra of DV-Chl *a* and MV-Chl *a* measured in acetone-d_6 at 273 K. Signals corresponding to ^{13}C atoms of the molecules are labeled. The peak at 30-32 ppm is acetone.

H) in the spectra of MV-Chls *a* were absent from the spectrum of DV-Chl *a*. Instead, the signals derived from 8-vinylic protons were observed at 8.180 ppm (dd, 8^1-H), 6.237 ppm (d, 8^2-H,) and 6.019 ppm (d, 8^2-H,) in the spectrum of DV-Chl *a*, as well as the signals of 3-vinylic protons at 8.291 ppm (dd, 3^1-H), 6.438 ppm (d, 3^2-H) and 6.266 ppm (d, 3^2-H); the latter signals in the spectrum of MV-Chls *a* appeared at 8.162 ppm (dd, 3^1-H), 6.242 ppm (dd, 3^2-H) and 6.028 ppm (dd, 3^2-H), respectively. The results confirm that 8-CH_2CH_3 of Chl *a* is substituted by –CH=CH_2 in DV-Chl *a*. No other clear changes are observed in the one-dimensional ^{1}H-NMR spectra.

B: ^{13}C-NMR

In the ^{13}C-NMR spectra (Fig. 7, Table 2), marked differences are noted in the range of 0 ppm to 20 ppm and 120 ppm to 140 ppm, relating to the –CH_2CH_3 and –CH=CH_2 moieties. Compared to MV-Chl *a*, the ^{13}C signals of 8-CH_2CH_3 were absent in the spectrum of DV-Chl *a*, while new 8-CH=CH_3 carbon signals appeared at 131 ppm (8^1-C) and 121 ppm (8^2-C), respectively, as well as the 3-CH=CH_3 carbon signals (130 ppm (3^1-C) and 124 ppm (3^2-C)), similar to Chl *a* (131 ppm (3^1-C) and 120 ppm (3^2-

Table 1. ^{1}H-chemcal shifts of Chl *a* and DV-Chl *a* in acetone-d_6 at 273K

IUPAC no.of carbon atom	Chl *a*	DV-Chl *a*	IUPAC no.of carbon atom	Chl *a*	DV-Chl *a*
2^1	3.343 (s)	3.511	P1	4.342 ,4.224	4.277, 4.228
3^1	8.162 (dd)	8.291 (dd)	P2	4.955	4.829
3^2	6.242 (dd), 6.028 (dd)	6.438 (d), 6.266 (d)	$P3^1$	1.509	1.52
5	9.410 (s)	9.679	P4	1.822	1.85
7^1	3.300 (s)	3.439	P5	1.31	1.25
8^1	3.817 (q)	8.180 (dd)	P6	0.97,1.17	1.01-0.93
8^2	1.696 (t)	6.237 (d), 6.019 (d)	P7	1.31	1.33
10	9.749 (s)	9.995	$P7^1$	0.811, 0.803	0.81, 0.81
12^1	3.619 (s)	3.709(s)	P8	1.01,1.23	1.01-0.93
13^2	6.234 (s)	6.406	P9	1.15,1.28	1.15
13^4	3.829 (s)	3.882	P10	1.01,1.23	1.01-0.93
17	4.175	4.037	P11	1.31	1.31
17^1	2.589 , 2.461	2.674, 2.619	$P11^1$	0.783, 0.774	0.79, 0.78
17^2	2.431 , 2.159	2.610, 2.539	P12	1.01,1.23	1.01-0.93
18	4.572 (q)	4.691	P13	1.23,1.28	1.18
18^1	1.772 , 1.762 (d)	1.855, 1.845(d)	P14	1.12	1.12
20	8.582 (s)	9.009	P15	1.500	1.58
			$P15^1$	0.854, 0.845	0.85, 0.85
			P16	0.854, 0.845	0.85, 0.85

Table 2. ^{13}C-chemcal shifts of Chl *a* and DV-Chl *a* in acetone-d_6 at 273K

IUPAC no. of carbon atom	Chl *a*	DV-Chl *a*	IUPAC no. of carbon atom	Chl *a*	DV-Chl *a*
1	155.47	155.66	17	50.98	52.08
2	136.28	133.35	17^1	30.28	29.51
2^1	12.65	12.38	17^2	30.66	30.66
3	139.76	138.46	17^3	173.29	173.18
3^1	131.30	129.92	18	49.73	50.70
3^2	120.33	123.67	18^1	23.01	24.37
4	148.96	142.36	19	169.69	169.02
5	100.58	98.42	20	93.78	94.91
6	152.78	152.11	P1	61.31	61.31
7	134.68	135.39	P2	120.17	119.11
7^1	11.15	12.75	P3	142.46	142.36
8	145.08	138.46	$P3^1$	16.11	16.12
8^1	19.91	130.898	P4	40.19	40.21
8^2	18.12	120.399	P5	25.54	25.60
9	146.74	142.359	P6	37.11	37.13
10	108.50	106.50	P7	33.43	33.44
11	148.34	148.78	$P7^1$	20.03	20.03
12	134.57	135.52	P8	37.94	38.02, 37.96, 37.89
12^1	12.65	11.74	P9	25.04	25.05
13	131.53	131.63	P10	38.01	38.02, 37.96, 37.89
13^1	190.30	174.72	P11	33.22	33.24
13^2	66.00	65.43	$P11^1$	19.98	19.86
13^3	171.32	173.10	P12	37.87	38.02, 37.96, 37.89
13^4	52.67	53.08	P13	25.49	25.49
14	162.55	167.98	P14	40.00	40.01
15	106.35	105.84	P15	28.65	28.66
16	156.50	157.40	$P15^1$	23.01^1	23.01
			P16	22.90^1	22.91

[1] assignment interchangeable

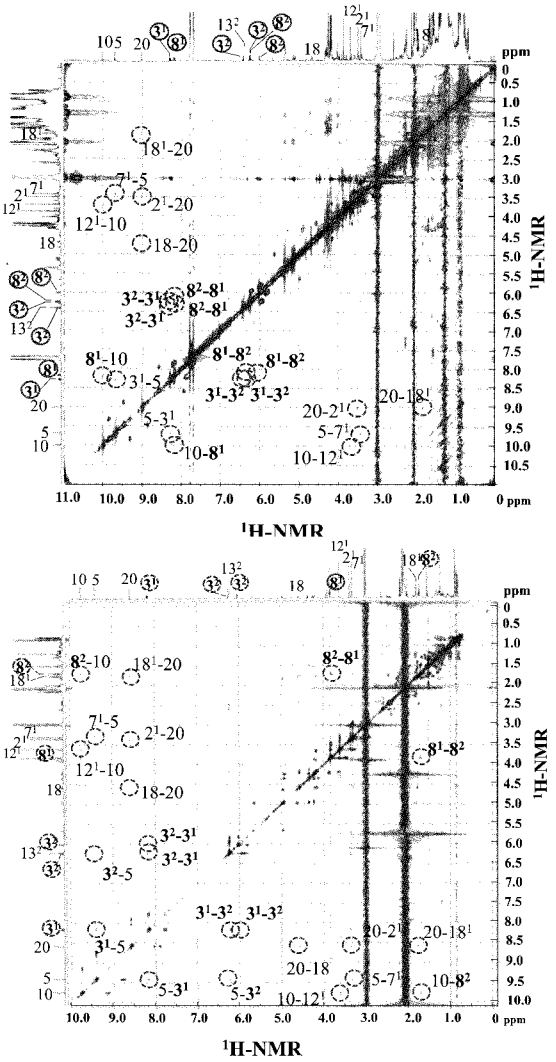

Fig. 8 ^{1}H-^{1}H NOESY spectra of DV-Chl *a* (top) and MV-Chl *a* (bottom) measured in acetone-d_6 at 273 K.

C)). Further remarkable differences are not seen in the one-dimensional ^{13}C-NMR spectra.

C: NOESY

As shown in Fig. 8, coherent correlations can be easily traced from 3^1-H of $-CH=CH_2$ on the NOESY spectra, where the signal of 3^1-H at 8.291 ppm on the NOESY spectrum of DV-Chl *a* showed two cross peaks with the signals of 3^2-H at 6.438 ppm and 6.266 ppm, respectively, while the signal of 3^1-H at 8.162 ppm on the MV-Chl *a* spectrum also possesses two cross peaks with the corresponding signal in the similar region, at 6.242 ppm and 6.028 ppm. As expected, good coherent correlations can also be traced from 8^1-H, but the position of cross peaks are completely different from each other; in DV-Chl *a* the signal of 8^1-H of $-CH=CH_2$ at 8.180 ppm showed two cross peak with the signal of 8^2-H at 6.237 ppm and 6.019 ppm, respectively, whereas in MV-Chl *a* the signal of 8^1-H of $-CH_2CH_3$ at 3.817 ppm exhibited a single cross peak with the signal of 8^2-H at 1.696 ppm and hence its cross peak position appeared far away area of the two cross peaks of DV-Chl *a*.

D: HSQC

As illustrated in the ^{1}H-^{13}C HSQC spectra of DV-Chl *a* and MV-Chl *a* (Fig. 9), all substituents on the macrocycle showed the corresponding cross peaks. As can be easily seen, three cross peaks associated with 3^1-3^1 and 3^2-3^2 of $-CH=CH_2$ in both DV-Chl *a* and MV-Chl *a* appeared in the same area (in the lower left corner of Fig. 9), but the area and number of 8^1-8^1 and 8^2-8^2 cross peaks were completely different, where three cross peaks in DV-Chl *a* in the lower left corner, but two cross peaks in MV-Chl *a* in the upper right corner of Fig. 9. Other cross peaks were seen in a similar area. The results support that 8-CH_2CH_3 of Chl *a* is replaced with $-CH=CH_2$ in DV-Chl *a*.

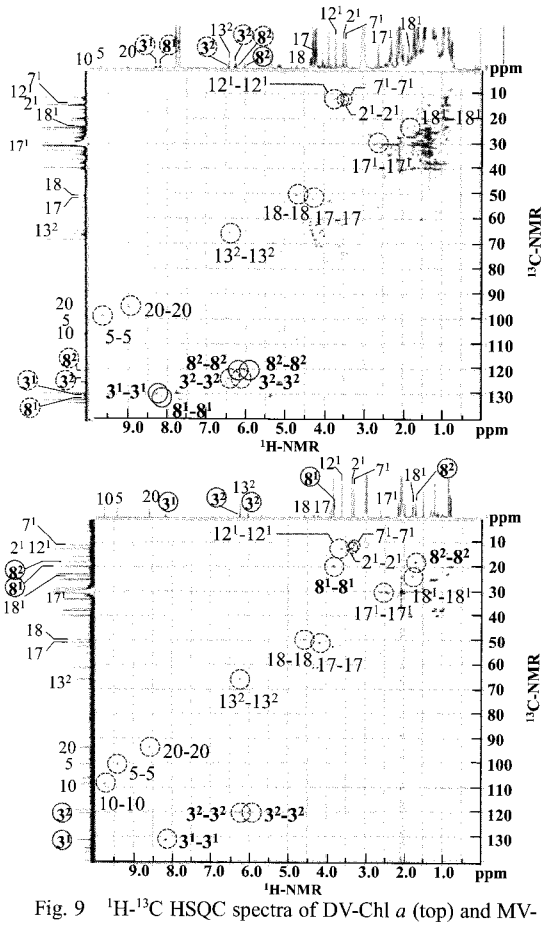

Fig. 9 ^{1}H-^{13}C HSQC spectra of DV-Chl *a* (top) and MV-Chl *a* (bottom) measured in acetone-d_6 at 273 K.

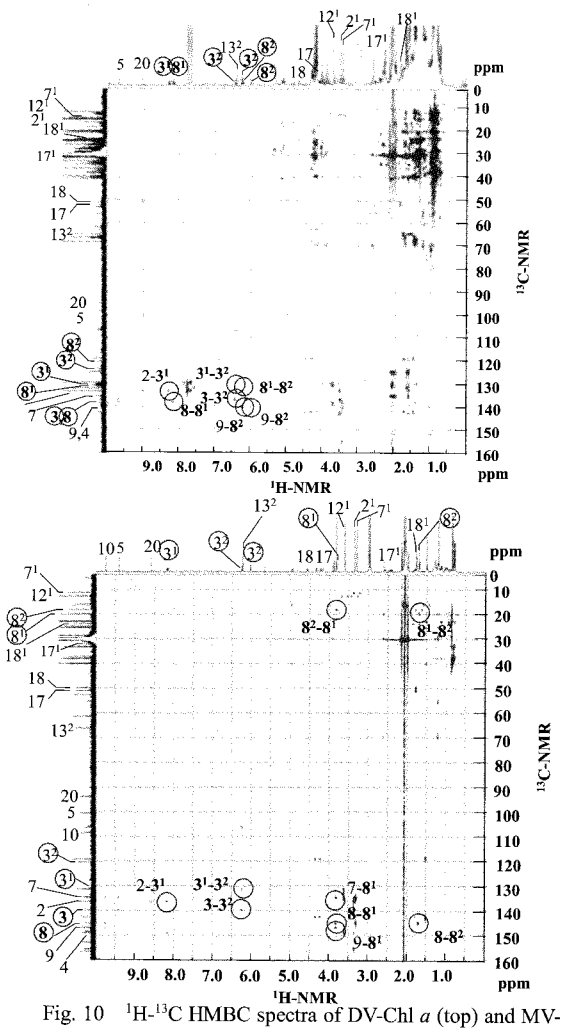

Fig. 10 ^{1}H-^{13}C HMBC spectra of DV-Chl *a* (top) and MV-Chl *a* (bottom) measured in acetone-d_6 at 273 K.

E: HMBC

HMBC also allows for the determination of connectivity between two different nuclear species as HSQC, but HMBC gives longer range coupling (2-4 bond coupling) than HSQC. In the ^{1}H-^{13}C HMBC spectrum of MV- and DV-Chls *a* (Fig. 10), the 3^{1}-H signal for –CH=CH$_2$ had one cross peak associated with the signal of 2-C, and the corresponding 3^{2}-H signal two cross peaks with the signals for 2-C and 3-C carbons. In the spectrum of DV-Chl *a*, the signal of an 8^{1}-vinilic hydrogen showed a cross peak with the signal of 8-C, while one of the signals of two 8^{2}-vinilic hydrogens had a cross peak with the signal of 8^{1}-C, and each signal of two 8^{2}-vinilic hydrogens possessed a cross peak with the signal of 9-C. In contrast, the 8^{1}-H signal for –CH$_2$-CH$_3$ in MV-Chl *a* exhibited four cross peaks; one is associated with the signal for 7-C, one is with the signal for 8-C, one is with the signal for 9-C, and the other is with the signal for 8^{2}-C carbon, whereas the 8^{2}-H signal had two cross peaks; one is with 8-C and the other with 8^{1}-C, respectively.

Redox potentials

As easily seen in the very similar absorption spectra of DV-Chl *a* and MV-Chl *a*, the redox potential difference between them can be expected to be very small. Signal-to-noise ratio of square wave voltammetry (SWV) is generally better than that of cyclic voltammetry (Cotton and Van Duyne 1979; Wasielewski *et al.* 1980; Kobayashi *et al.* 2007), and hence we measured their redox potentials by means of SWV.

Typical SWVs for DV-Chl *a* and MV-Chl *a* in acetonitrile are illustrated in Fig. 11. Four well separated peaks were observed in each voltammogram, and the potentials in anodic sweep and cathodic sweep (data not shown) are identical to each other, indicating that the four redox reactions are reversible. As expected, redox potential difference between DV-Chl *a* and MV-Chl *a* was very much small; DV-Chl *a* showed slightly more positive oxidation potentials than MV-Chl *a* only by 8 mV. The redox potentials of chlorophylls are sensibly affected by the nature of substituent groups on the π-electron system (Fuhrhop 1975; Watanabe and Kobayashi 1991; Kobayashi *et al.* 2007). As expected from the inductive effect of substituent groups, replacement of ←CH$_2$-CH$_3$ at C8 the macrocycle to be electron poor, thus rendering the molecule less oxidizable (first oxidation potential, E^{1}_{ox}: DV-Chl *a* > MV-Chl *a*). Slightly less negative first reduction potential, E^{1}_{red}, observed in DV-Chl *a* of MV-Chl *a* by –CH=CH$_2$ to yield DV-Chl *a* causes than that of MV-Chl *a* by 10 mV can be also explained in a

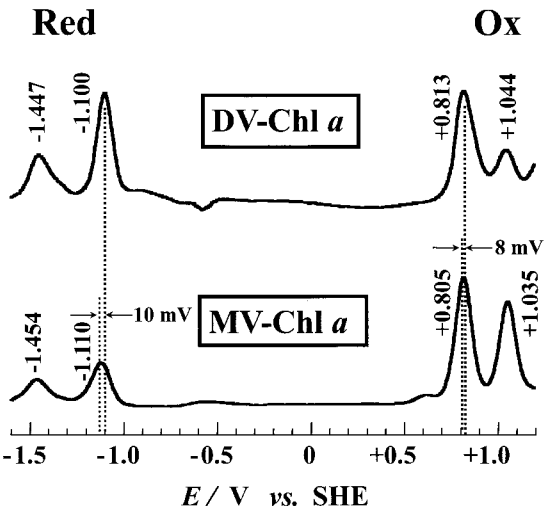

Fig. 11 Square wave voltammograms of DV-Chl *a* and MV-Chl *a* in acetonitrile at room temperature.

similar way, namely, replacement of $\leftarrow CH_2\text{-}CH_3$ by $-CH{=}CH_2$ causes the macrocycle to be electron poor, thus rendering the molecule more easily reduced.

The redox behavior of a compound is related to the energy levels of its molecular orbitals: E^1_{ox} is intimately related to the highest occupied molecular orbital (HOMO) and E^1_{red} to the lowest unoccupied molecular orbital (LUMO), and hence the primary redox potential difference, $\Delta E = E^1_{ox} - E^1_{red}$, can be taken as an index for the Q_Y excitation energy (Watanabe and Kobayashi 1991; Hanson 1991; Kobayashi *et al.* 2007, 2013). Almost the same value of ΔE for DV-Chl *a* and MV-Chl *a* correlates to the practically identical Q_Y excitation wavelengths as seen in Figs.3 (top) and 4A', B'.

Conclusion

The essential physicochemical properties (normal-phase and reversed-phase HPLC elution profiles, visible absorption spectra in four organic solvents, CD spectra, MS spectra, one-dimensional and two-dimensional NMR spectra and redox potential) of DV-Chl *a* as well as DV-Chl *a'* and DV-Phe *a* are systematically compared for the first time with those of normal chlorophylls, namely, MV-Chl *a* and its derivatives. Unexpectedly many differences are found, which will help to clarify the unexplained photomechanisms of DV-type photosynthesis.

Acknowledgements

We thank Dr. Nobuaki Ishida (Ishikawa Prefectural Univ.) for his kind and invaluable help. This work was supported in part by Special Project of Organization for the Support and Development of Strategic Initiatives (Green Innovation) (Univ. Tsukuba) to M.K.

References

Bazzaz MB (1981) New chlorophyll chromophores isolated from a chlorophyll deficient mutant of maize. *Photobiochem. Photobiophys.*, **2**: 199-207.

Bazzaz MB and Brereton RG (1982) 4-vinyl-4-desethyl chlorophyll *a*: a new naturally occurring chlorophyll. *FEBS Lett.*, **138**: 104-108.

Bidigare RR and Ondrusek ME (1996) Spatial and temporal variability of phytoplankton pigment distributions in the central equatorial Pacific Ocean. *Deep-Sea Res. II*, **43**: 809-833.

Campbell L, Nolla HA and Vaulot D (1994) The importance of Prochlorococcus to community structure in the central North Pacific Ocean. *Limnol. Oceanogr.*, **39**: 954-961.

Chisholm SW, Olson RJ, Zettler ER, Goericke R, Waterbury JB and Welschmeyer NA (1988) A novel free-living prochlorophyte abundant in the oceanic euphotic zone. *Nature*, **334**: 340-343.

Cotton TM and Van Duyne RP (1979) Electrochemical investigation of the redox properties of bacteriochlorophyll and bacteriopheophytin in appoticsolvents, *J. Am. Chem. Soc.*, **101**: 7605–7612.

Eskins K, Scholfield CR and Dutton HJ (1977) High-performance liquid chromatography of plant pigments. *J. Chromatogr.* **135**: 217-220.

Fuhrhop JH (1975) Reversible reactions of porphyrins and metalloporphyrins and electrochemistry. in *Porphyrins and Metalloporphyrins*, ed. by Smith KM, Elsevier, Amsterdam, Chapter 14.

Fujinuma D, Akutsu S, Komatsu H, Watanabe T, Miyashita H, Islam MR, Koike H, Kawachi M, and Kobayashi M (2012) Detection of divinyl chlorophyll *a'* and divinyl pheophytin *a* in a marine picoplankton *Prochlorococcus* sp. RCC315, *Photomed. Photobiol.*, **34**: 47-52.

Gieskes WW and Kraay GW (1983) Unknown chlorophyll a derivatives in the North Sea and the tropical Atlantic Ocean revealed by HPLC analysis. *Limnol. Oceanogr.*, **28**: 757-766.

Gieskes WW and Kraay GW (1986) Floristic and physiological differences between the shallow and the deep nanoplankton community in the euphotic zone of the open tropical Atlantic revealed by HPLC analysis of pigments. *Mar. Biol.*, **91**: 567-576.

Goericke R and Repeta DJ (1993) Chlorophylls *a* and *b* and divinyl chlorophylls *a* and *b* in the open subtropical North Atlantic Ocean. *Marine Ecology Progress Series*, **101**: 307-313

Gouterman M (1961) Spectra of porphyrins. *J. Mol. Spectrosc.*, **6**: 138-163.

Gouterman M, Wagniere GH and Snyder LC (1963) Spectra of porphyrins : part II. Four orbital model. *J. Mol. Spectrosc.*, **11**: 108-127.

Hanson LK (1991) Molecular orbital theory on monomer pigments. In *Chlorophylls*, ed. by Scheer H, CRC Press, Boca Raton, Florida, pp.993-1014.

Islam MR, Aikawa S, Midorikawa T, Kashino Y, Satoh K, and Koike H (2008) *slr*1923 of *Synechocystis* sp. PCC6803 is essential for conversion of 3,8-divinyl(proto)chlorophyll(ide) to 3-monovinyl(proto)chlorophyll(ide)[1], *Plant Physiol.*, **148**: pp. 1068–1081.

Jayaraman S, Knuth ML, Cantwell M and Santos A (2011)

High performance liquid chromatographic analysis of phytoplankton pigments using a C_{16}-Amide column. *Journal of chromatography A*, **1218**: 3432-3438.

Jeffrey SW and Humphrey GF (1975) New spectrophotometric equations for determining chlorophylls *a, b, c1* and *c2* in higher plants, algae and natural phytoplankton. *Biochem. Physiol. Pflanz.*, **167**: 191-194.

Jeffrey SW, Wright SW and Zapata M (1999) Recent advances in HPLC pigment analysis of phytoplankton. *Mar. Freshwat. Res.*, **50**: 879-896.

Jordan P, Fromme P, Witt HT, Klukas O, Saenger W and Krauβ N (2001) Three-dimensional structure of cyanobacterial photosystem I at 2.5 Å resolution. *Nature*, **411**:909-917.

Klimov VV, Klevanik AV, Shuvalov VA and Krasnovsky AA (1977a) Reduction of pheophytin in the primary light reaction of photosystem II. *FEBS Lett.*, **82**: 183-186.

Klimov VV, Allkhverdiev SI, Demeter S and Krasnovsky AA (1977b) Photoreduction of pheophytin in photosystem 2 of chloroplasts with respect to the redox potential of the medium. *Dokl. Akad. Nauk SSSR*, **249**: 227-230.

Kobayashi M, Watanabe T, Nakazato M, Ikegami I, Hiyama T, Matsunaga T and Murata N (1988) Chlorophyll *a'*/P700 and pheophytin *a*/P680 stoichiometries in higher plants and cyanobacteria determined by HPLC analysis. *Biochim. Biophys. Acta* **936**: 81-89.

Kobayashi M, van de Meent EJ, Erkelens, Amesz J, Ikegami I and Watanabe T (1991) Bacteriochlorophyll *g* epimer as a possible reaction center component of heliobacteria. *Biochim. Biophys. Acta* **1057**: 89-96

Kobayashi M, Akiyama M, Kano H and Kise H (2006) Spectroscopy and structure determination. In *Chlorophylls and Bacteriochlorophylls: Biochemistry, Biophysics, Functions and Applications*, ed. by Grimm B, Porra RJ, Rüdiger W and Scheer H, Springer, Dordrecht, The Netherlands, pp.79-94.

Kobayashi M, Ohashi S, Iwamoto K, Shiraiwa Y, Kato Y and Watanabe T (2007) Redox potential of chlorophyll *d in vitro*. *Biochim. Biophys. Acta* **1767**:596-602.

Kobayashi M, Akutsu S, Fujinuma D, Furukawa D, K omatsu H, Hotota Y, Kato Y, Kuroiwa Y, Watana be T, Ohnishi-Kameyama M, Ono H, Ohkubo S and Miyashita H (2013) Physicochemical Properti es of Chlorophylls in Oxygenic Photosynthesis–Su ccession of co-factors from anoxygenic to oxygen ic photosynthesis. In *Photosynthesis*, ed. by Z. D ubinsky, Intech, Croatia, Chapter 3, pp. 47-90 (http://dx.doi.org/10.5772/55460).

Latasa M, Bidigare RR, Ondrusek ME, and Kennicutt II MC (1996) HPLC analysis of algal pigments: a comparison exercise among laboratories and recommendations for improved analytical performance. *Marine Chemistry.*, **51**: 315-324.

Letelier RM, Bidigare RR, Hebel DV, Ondrusek M, Winn CD and Karl DM (1993) Temporal variability of phytoplankton community structure based on pigment analysis. *Limnol. Oceanogr.*, **38**: 1420-1437.

Moore LR, Post AF, Rocap G, and Chisholm SW (2002) Utilization of different nitrogen sources by the marine cyanobacteria *Prochlorococcus* and *Synechococcus*. *Limnol. Oceanogr.*, **47**(4): 989–996

Petke JD, Maggiora GM, Shipman L and Christoffersen RE (1979) Stereoelectronic Properties of Photosynthetic and related systems - v. *ab initio* configuration interaction calculations on the ground and lower excited singlet and triplet states of ethyl chlorophyllide *a* and ethyl pheophorbide *a*. *Photochem. Photobiol.* **30**: 203-223.

Schoch S (1978) The esterification of chlorophyllide *a* in greening bean leaves. *Z . Naturforsch., C: Biosci.*, **33C**: 712-714.

Shoaf WT (1978) Rapid method for the separation of chlorophylls *a* and *b* by high-pressure liquid chromatography. *J. Chromatogr.*, **152**: 247-249.

Tomo T, Akimoto S, Ito H, Tsuchiya T, Fukuya M, Tanaka A and Mimuro M (2009) Replacement of chlorophyll with di-vinyl chlorophyll in the antenna and reaction center complexes of the cyanobacterium *Synechocystis* sp. PCC 6803: Characterization of spectral and photochemical properties. *Biochimica et Biophysica Acta*, **1787**:191-200.

Van Heukelem L and Thomas CS (2001) Computer-assisted high-performance liquid chromatography method development with applications to the isolation and analysis of phytoplankton pigments. *Journal of Chromatography A*, **910**: 31-49.

Wasielewski MR, Smith RL, and Kostka AG (1980) Electrochemical production of chlorophyll *a* and pheophytin *a* excited states. *J. Am. Chem. Soc.*, **102**: 6923-6928.

Watanabe T, Hongu A, Honda K, Nakazato M, Konno M and Saitoh S (1984) Preparation of chlorophylls and pheophytins by isocratic liquid chromatography. *Anal. Sci.*, **56**: 251-256.

Watanabe T and Kobayashi M (1991) Electrochemistry of chlorophylls. In *Chlorophylls*, ed. by Scheer H, CRC Press, Boca Raton, pp. 287–315.

Weiss C (1978) Electronic absorption spectra of chlorophylls. In *The Porphyrins,* Vol. III, Physical Chemistry, Part A, ed. by Dolphin D, Academic Press, New York, pp 211-223.

Wolf H and Scheer H (1973) Stereochemistry and chiroptic properties of pheophorbides and related compounds. *Ann. N. Y. Acad. Sci.*, **206**: 549-567.

Wright SW, Jeffrey SW, Mantoura RFC, Llewellyn CA, Bjørnland T, Repeta D and Welschmeyer N (1991) Improved HPLC method for the analysis of chlorophylls and carotenoids from marine phytoplankton. *Mar. Ecol. Prog. Ser.*, **77**: 183-196.

Zapata M, Rodríguez F and Garrido JL (2000) Separation of chlorophylls and carotenoids from marine phytoplankton: a new HPLC method using a reversed phase C_8 column and pyridine-containing mobile phases. *Mar. Ecol. Prog. Ser.*, **195**: 29-45.

Zouni A, Witt HT, Kern J, Fromme P, Krauβ N, Saenger W and Orth P (2001) Crystal structure of Photosystem II from *synechococcus elongates* at 3.8 Å resolution. *Nature,* **409**: 739-743.